RESEARCH ARTICLE

Biosilica 3D Micromorphology of Geodiidae Sponge Spicules Is Patterned by F-Actin

Alona Voronkina[1,2] 🆔 | Paco Cárdenas[3] | Jörg Adam[2] | Heike Meissner[4] | Krzysztof Nowacki[5] | Yvonne Joseph[2] | Konstantin R. Tabachnick[6] | Hermann Ehrlich[7,8]

[1]Pharmacy Department, National Pirogov Memorial Medical University, Vinnytsia, Ukraine | [2]Institute for Nanoscale and Biobased Materials, TU Bergakademie Freiberg, Freiberg, Germany | [3]Pharmacognosy, Department of Pharmaceutical Biosciences, Museum of Evolution, Uppsala University, Uppsala, Sweden | [4]Department of Prosthetic Dentistry, Faculty of Medicine, Technische Universität Dresden, Dresden, Germany | [5]Institute of Chemistry and Technical Electrochemistry, Poznan University of Technology, Poznan, Poland | [6]INTIB Internationales Institut für Biomineralogie GmbH, Freiberg, Germany | [7]Center for Advanced Technology, Adam Mickiewicz University in Poznan, Poznan, Poland | [8]Institute of Chemical Technology, Faculty of Chemical Technology, Poznan University of Technology, Poznan, Poland

Correspondence: Paco Cárdenas (paco.cardenas@em.uu.se) | Hermann Ehrlich (hermann.ehrlich@amu.edu.pl)

ABSTRACT

Demosponges (phylum Porifera) are among the first multicellular organisms on the planet and represent a unique archive of biosilica-based skeletal structures with species-specific microstructures called spicules. With more than 80 morphotypes, this class of sponges is recognized as a unique source of amorphous silica with superficial ornamentation patterned by organic phases. In this study, we investigated spicules of selected representatives of the family Geodiidae (order Tetractinellida), to identify F-actin-containing axial filaments within these 3D skeletal microconstructs defined as oxyspherasters and sterrasters. Their desilicification using 10% HF leads to isolation of multifilamentous, radially oriented organic matrices, which resemble the shape and size of the original spicules. Our data show that highly specific indicators of F-actin such as iFluorTM 594-Phalloidin, iFluorTM 488-Phalloidin, as well as iFluorTM 350-Phalloidin unambiguously confirm its localization within demineralized oxyspherasters and sterrasters of 11 diverse demosponges species belonging to the subfamily Geodiinae (genera *Geodia*, *Rhabdastrella*) and the subfamily Erylinae (genera *Caminella*, *Caminus*, *Erylus*, *Pachymatisma*). Well-defined periodicity in *Geodia cydonium* sterrasters actin filaments has been observed using atomic force microscopy (AFM) for the first time. The findings of F-actin as a possible pattern driver in spicules of geodiids brings additional light to our knowledge of spiculogenesis in this group. However, no specific actin structures were found between the geodiid subfamilies or genera thereby suggesting a common actin process, present already at the emergence of the family (~170 million years ago).

1 | Introduction

Sponges (phylum Porifera), present at least since the Early Cambrian (Chang et al. 2019), represent a unique biomineralogical archive in terms of the diversity of their skeletons and corresponding structural formations. These structures are made of calcium carbonates (class Calcarea), biosilica (class Demospongiae and Homoscleromorpha), or both biomineral phases (class Hexactinellida) (Ehrlich et al. 2011). Most of these structures are characterized by their size, their shape, and their

Summary

- F-actin patterns the microstructured biosilica in 11 diverse species of demosponges.
- Actin filaments in siliceous sterrasters possess radially oriented organization.
- Multifilament actin-based aggregates with a well-defined periodicity have been observed.
- An actin pattering process is common to the whole geodiid sponges family during 170 MYR.

superficial ornamentations; there are more than 46 and 80 morphotypes in Hexactinellida and Demospongiae, respectively (Łukowiak 2020; Łukowiak et al. 2022; Uriz et al. 2003). However, patterning mechanisms leading to the diversity of size/shape as well as network connectivity in the form of unique monaxons, triaxons, or tetraxons are still poorly understood (Łukowiak et al. 2022). The possible templating activity of the axial filament in general (Görlich et al. 2020; Schoeppler et al. 2017) and the more specific roles of collagen (Ehrlich et al. 2010), chitin (Ehrlich et al. 2016), glassin (Shimizu et al. 2015), hexaxilin, perisilin (Shimizu et al. 2024), silicateins (Görlich et al. 2020; Wang et al. 2010) and, as recently reported actin (Ehrlich et al. 2022; Voronkina et al. 2023), remain under study. The role of actin in biosilicification is still poorly investigated, despite the fact that actin has been experimentally confirmed as the crucial element in the control of the silica morphogenesis at the meso- and microscale in numerous diatoms (Tesson and Hildebrand 2010).

Sponges from the family Geodiidae (order Tetractinellida) are present at least since the Middle Jurassic some 170 Mya (Cárdenas 2020) and are today found worldwide, except in Antarctic waters. They are for the most part massive subspherical sponges, some of which dominate in terms of size and biomass boreo-arctic sponge grounds in the North Atlantic (Cárdenas et al. 2013; Klitgaard and Tendal 2004). Geodiidae species present one of the richest diversity of siliceous spicules among the demosponges. One species of *Geodia* can commonly present up to three or four types of megascleres (large spicules, millimeter in size) in combination with up to four types of microscleres (small spicules, micrometer in size) (Cárdenas et al. 2013). Perhaps, the most striking of these spicules are the ball-shaped sterrasters (30–560 μm) with their intricate surface microornamentations. These structures may be used by fibers to solidly link sterrasters with each other (Cárdenas 2020) thus forming a dense layer of spicules and tough physical protection against predation. These sterrasters have evolved differently in different Geodiidae clades and may have in fact appeared independently at least three times (Cárdenas 2020). They were also secondarily lost on many occasions throughout evolution (Cárdenas et al. 2010, 2011).

Genesis of these sterraster spicules is complex and documented early on by Sollas (1880) using a light microscope. Scanning electron microscopy and synchrotron micro/nanotomography have enabled more detailed observations of the process (Rützler and Macintyre 1978; Schoeppler et al. 2017). In brief, microscleres such as sterrasters are

produced inside specific sclerocytes by a polyaxial filament producing polyactine star-shaped spicules with every branch (=actine) supported by a proteinaceous axial filament containing only silicatein-α/β (Cárdenas and Rapp 2013; Müller et al. 2007; Rützler and Macintyre 1978; Simpson 1989). The space between the actines is then filled with silica, deposited in layers, supposedly by the so-called silicalemma (an evagination of the plasmalemma), giving the hedgehog- or morula-shaped stage (Cárdenas and Rapp 2013; Rützler and Macintyre 1978). At this point, a second silicification process, maybe also involving the silicalemma, takes place producing the microornamentations, small star-shaped structures called "rosettes" at the tips of every actine (Cárdenas and Rapp 2013; Rützler and Macintyre 1978). During or after this process, mature sterrasters are transported to the surface of the animal by the sclerocytes and released there where they will be integrated into the cortex (Sollas 1880). Short axial filaments are also involved in shaping the surface microornamentations, supposedly one per "extension" (Cárdenas and Rapp 2013; Simpson 1989).

It is usually considered that the proteinaceous axial filaments guide spicule morphology (Pisera 2003; Schoeppler et al. 2017) thanks to their hybrid protein/silica crystal structure (Görlich et al. 2020). The role of actin filaments in several Hexactinellida and Demospongiae (Ehrlich et al. 2022) has been put forward as guiding structures for biosilicification and 3D constructs. Ehrlich et al. (2022) (Figure 1B, Figure S10) thus revealed the presence of actin in sterrasters of *Geodia cydonium*. The purpose of this study was to further investigate the morphology and structure of actin filaments in sterrasters with an evolutionary perspective and investigate their potential role in sterraster spiculogenesis.

2 | Materials and Methods

2.1 | Biological Samples Origin

A series of species belonging to the family Geodiidae were selected based on the production of sterraster microscleres. One exception is the genera *Rhabdastrella* that has large oxyspherasters (star-shaped microsclere) instead of sterrasters. Traditionally classified in the Ancorinidae, molecular phylogenetic studies have suggested that *Rhabdastrella* belongs to the Geodiidae instead. Species came from the subfamily Geodiinae (genera *Geodia, Rhabdastrella*) and the subfamily Erylinae (genera *Caminella, Caminus, Erylus, Pachymatisma*). Samples came from the Museum of Evolution, Uppsala, Sweden (UPSZMC), the Bergen Museum, Bergen, Norway (ZMBN) and one from the University of California Museum of Paleontology, Berkeley, USA (UCMPW). A total of 11 species were investigated: *Caminella intuta* Topsent 1892, UPSZMC 191586, Gameau cave, La Ciotat, France, 43°9.876′ N, 05°35.934′ E, 16 m; *Caminus vulcani* Schmidt, 1862, UPSZMC 190811 (i391-2), Emile Baudot Seamount, Mallorca Channel, 38°42′56″ N, 2°29′11″ E, 146 m; *Erylus euastrum* Schmidt 1868, UPSZMC 191971 (PC631), Capo Rizzuto, Calabria, Italy, 39°10.802′ N, 17°15.543′ E, 150 m; *Erylus formosus* Sollas 1886, ZMBN 82978 (PC36), Little Salvador Island, Bahamas; *Erylus granularis* Topsent 1904, UPSZMC 191573 (PC1384),
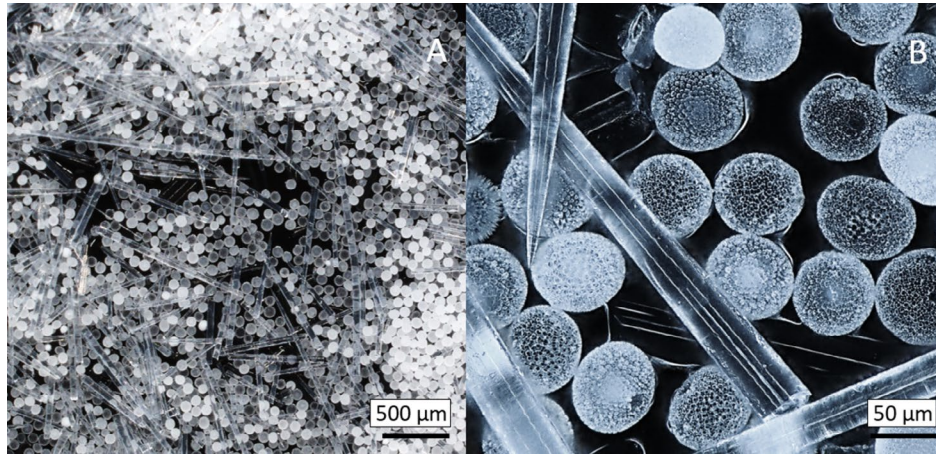
FIGURE 1 | Digital optical microscopic images of *Geodia cydonium* siliceous spicules. (A) Megascleres (oxeas, and microscleres (sterrasters)). (B) Close-up on (A) showing oxea fragments and ball-shaped sterrasters.

Rosemary Bank, Rockall Trough, 59°6.906′N, 10°52.128′W, 1405 m; *Geodia barretti* Bowerbank 1858, UPSZMC 184976 (PC980), Kosterfjord, Sweden, 58°52.574′N, 11°06.089′E, 96 m; *G. cydonium* Linnaeus 1767, Cave Coral, Maïre Island, Marseille, France, 43°12′37.60″N, 5°20′24.86″E; *Geodia macandrewii* Bowerbank 1858, ZMBN 89718 (PC510), Svalbard, 80°32.3115′N, 15°21.69708′E, 215 m; *Geodia phlegraei* Sollas 1880, ZMBN 89719 (PC511), Svalbard, 80°32.3115′N, 15°21.69708′E, 215 m; *Pachymatisma normani* Sollas 1888, UPSZMC 191572 (PC196), Røst reef, Norway, 67°30.10′N, 9°24.5′E, 301 m; *Rhabdastrella globostellata* Carter 1883, UCMPW 1072 (PC140), near Manus Island, northwest coast of New Ireland, Papua New Guinea.

2.2 | Scanning Electron Microscopy (SEM)

The surface morphology and microstructure of the spicules and asters isolated from *G. cydonium* were analyzed using SEM images with a scanning electron microscope (XL 30 ESEM, Philips, Eindhoven, NL). Prior to scanning, the samples were coated with a gold layer using the Cressington Sputtercoater 108 auto, Crawley (GB) (sputtering time 45 s).

2.3 | Actin Isolation

The isolation of axial actin filaments from asters and spicules of all investigated sponges' samples was performed using the "sliding drop technique" (Ehrlich et al. 2022): selected spicules have first been treated with 70% HNO_3 (Sigma Aldrich) at room temperature for 72 h to remove possible organic impurities. Then spicules were rinsed in distilled H_2O up to pH 6.5, dried on air at room temperature, and placed on the Nunc Permanox (Thermo Fisher Scientific, USA) plastic microscope slides (27/75 mm) in small drops of water. After water evaporation, one drop of 10% HF acid (Ehrlich et al. 2022) was added to the sample, and the slide was placed inside the Plexiglas Petri dish at a 10° angle and closed for HF evaporation prevention. The samples were left for 7–10 h for silica dissolving. The residual demineralized axial filaments of spicules were then rinsed with water, dried in the air, and stored at 4°C.

2.4 | Digital Microscopy

Organic-free spicules before and after demineralization were observed using a Keyence VHX-7000 digital optical microscope with objectives VHX E20 (magnification up to 100×) and VHX E100 (magnification up to 500×) (Keyence, Osaka, Japan).

2.5 | Atomic Force Microscopy (AFM)

Organic-free demineralized sterraster spicules were analyzed with a TopoMetrix TMX-2010 scanning probe microscope using silicon cantilevers of type CSC12 (MikroMasch, Innovative Solutions Bulgaria Ltd.) in contact mode. No further sample preparation was necessary. Image processing was carried out using Gwyddion SPM data analysis software.

2.6 | Laser Scanning Microscopy (LSM)

Confocal topographic images of organic-free demineralized sterrasters were obtained with an Olympus LEXT OLS4100 3D Measuring Laser Microscope (Olympus Corporation, Japan), microscope objective type "MPLAPONLEXT 100x" with no further sample preparation.

2.7 | Phalloidin Staining

Cell Navigator F-Actin-labeling kits were used for demineralized spicules staining: *Red Fluorescence* iFluor 594-Phalloidin (Cat#22664), *Green Fluorescence* iFluor 488-Phalloidin (Cat#22661), *Blue Fluorescence* iFluor 350-Phalloidin (Cat#22660). For preparing the working solution for each staining kit 10 μL of iFluor Phalloidin (Component A) was added to 10 mL of Labeling buffer (Component B). To the fixed on the Nunc Permanox (Thermo Fisher Scientific) plastic microscope slides demineralized spicules samples, preliminarily treated with 1% BSA solution in DPBS for nonspecific phalloidin binding prevention (Buchwalow et al. 2011; Moreno et al. 2019), 100 μL/sample of iFluor Phalloidin

working solution was added. Samples were stained for 60 min at the room temperature in the dark place. Afterward, the plates were carefully washed five times with distilled water to remove excess dye, dried, and observed using fluorescent microscopy. Unused iFluor Phalloidin stock solutions were stored at −20°C and protected from light.

2.8 | Fluorescence Microscopy

Fluorescence microscopy images were obtained using the Keyence BZ-9000 digital optical microscope (Keyence, Osaka, Japan) with objectives CFI Plan Apo 10×, CFI Plan Apo 40×, CFI Plan Apo 100×H (Oil immersion) using DAPI channel (Ex/Em = 360/460 nm) for blue-stained samples (images presented in cyan), GFP channel (Ex/Em = 470/525) for green-stained samples, TxRed channel (Ex/Em = 560/630) for red-stained samples and the bright field for comparison. As a control, unstained samples of the same species were observed with the same exposure time (which varied from 1/30 to 1/12 s depending on the sample and the channel) used for the stained one via the same channel. The fluorescence of the stained samples was controlled using all mentioned channels.

3 | Results and Discussion

The digital microscopy and SEM of the material obtained after removing organic impurities from *G. cydonium* have shown siliceous sterrasters and spicules characteristic of the geodiid species (Figure 1, Figure 2A). The SEM analysis confirmed the presence of specific morphology of the *G. cydonium* sterrasters—warty rosettes (Cárdenas 2020) (Figure 2A). Different stages of sterraster spiculogenesis were present (Cárdenas and Rapp 2013) (Figure 2A), which allowed us to observe the axial canals inside the silicious structure (Figure 2B). The diameter of axial canals varied from 1.44 to 2.05 μm (Figure 2B). Some naturally poorly silicified sterrasters revealed the axial filaments in the surface rosettes (Figure 2C) and the whole sterrasters (Figure 2D).

After the desilicification process and washing of the samples, they lose their mechanical strength but retain the spherical structures formed by the axial filaments connected in the middle (Figures 3A,B, 4, and 6). The topography of these structures with heights of up to 2 μm is represented in Figure 4. These results confirm previous observations of demineralized sterrasters (fig 6 in Müller et al. 2007).
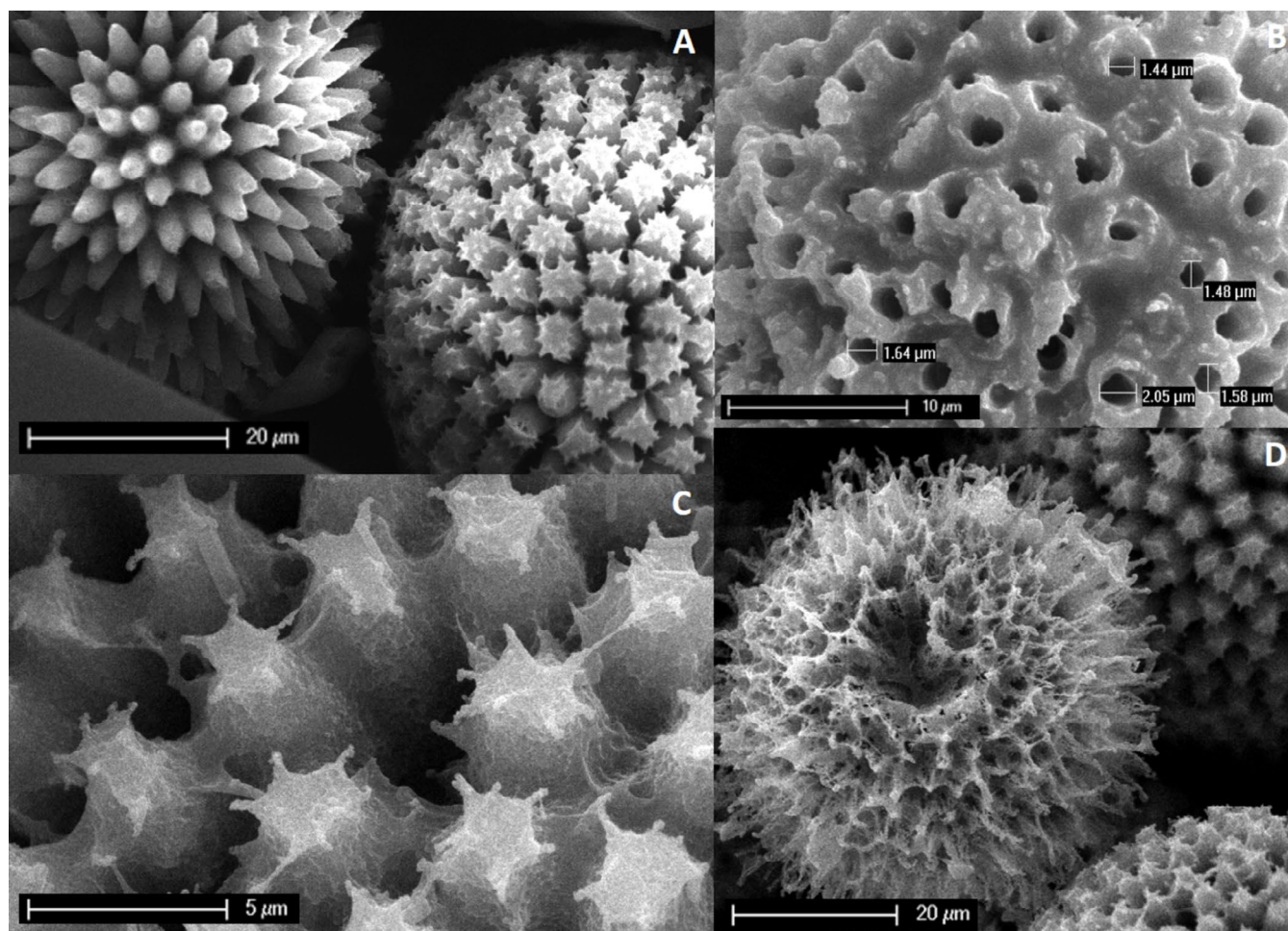
FIGURE 2 | SEM images of G. cydonium sterrasters (A) young stage (hedgehog stage) (right) and final stage (left) of sterraster. Note the microornamentations called rosettes present at the final stage. (B) Close-up of the surface of a developing sterraster showing the axial channels. (C) Close-up of underdeveloped sterraster showing incomplete poorly silicified rosettes. (D) Poorly silicified sterraster showing its internal structure with polyaxial filament.
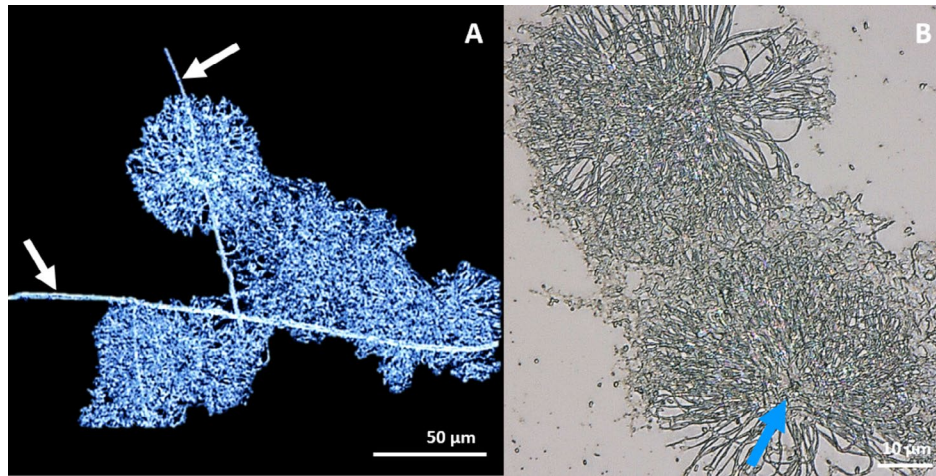
FIGURE 3 | Digital microscopic images of the axial filaments after *G. cydonium* sterrasters desilicification. (A) Both needle-like (arrows) and spherical structures are visible, remnants of oxeas and sterraster spicules. (B) The place of filaments connection (arrow) is clearly observed in these polyaxial filaments with radial orientation.
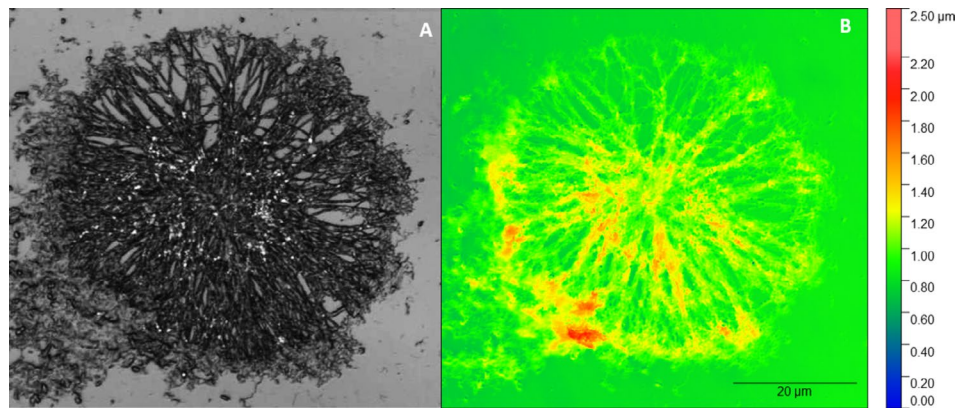
FIGURE 4 | Simultaneously made LSM pictures of the axial filaments with multiple branching after *G. cydonium* sterrasters desilicification: (A) intensity (grayscale) image, (B) topographic image (color scale indicates the height). Images were obtained under the same conditions, image section, and objective.

The "gold standard F-actin marker" phalloidin (Melak, Plessner, and Grosse 2017) is a bicyclic heptapeptide toxin of *Amanita phalloides* mushroom origin that is able to stoichiometrically bind to F-actin with high specificity (Pospich, Merino, and Raunser 2020). It stabilizes actin filaments and prevents depolymerization (Cano et al. 1992) even under harsh chemical conditions, that is, in formaldehyde-fixed, or paraffin-embedded samples (Dhakal, Black, and Mohanty 2014; Romani and Auwerx 2021). Phalloidin has also been successfully used for staining of actin filaments isolated from diverse skeletal structures of sponges treated with 10% HF (Ehrlich et al. 2022). In this study (Ehrlich et al. 2022), the presence of actin has been confirmed additionally to phalloidin-staining also using such recognized approaches as Raman spectroscopy, immunostaining with corresponding antibodies, western blotting techniques as well as inhibitors. Therefore, the use of phalloidins as indicators of actin does not raise doubts about its reliability (Han et al. 2023).

Staining of the *G. cydonium* demineralized sterrasters with phalloidin conjugated with different fluorochromes (red, green, and blue) resulted in the characteristic fluorescence (Figure 5A,C,E)

perfectly overlaying the shape of the polyaxial filaments observed in bright field (Figure 5B,D). The dense center is clearly visible (Figure 5A,E). The experimental samples under the same conditions exhibited fluorescence signals significantly higher than the negative controls, confirming the specificity of the F-actin staining.

Atomic force microscopy (AFM) remains another recognized method for the characterization of actin filaments, especially to image molecular assemblies of F-actin (Henderson, Haydon, and Sakaguchi 1992; Henderson and Sakaguchi 1993; Jung, Kim, and Mun 2020; Narita et al. 2016; Shao, Shi, and Somlyo 2000; Zhang et al. 2003). Our AFM images (Figure 6) showed segmentation patterns determined by nanostructures with a highly condensed appearance, which is a characteristic of F-actin including that of actin bundles (Gilmore, Kumeta, and Takeyasu 2013). The diameter of F-actin-based axial filaments of *G. cydonium* sterrasters measured in this study was 310–320 nm thick and 25–27 µm long. The number of actin filaments in demineralized sterrasters ranged between 300 and 400 (Figures 3–8) depending on the sponge species. To the best of our knowledge, this kind of periodicity has never
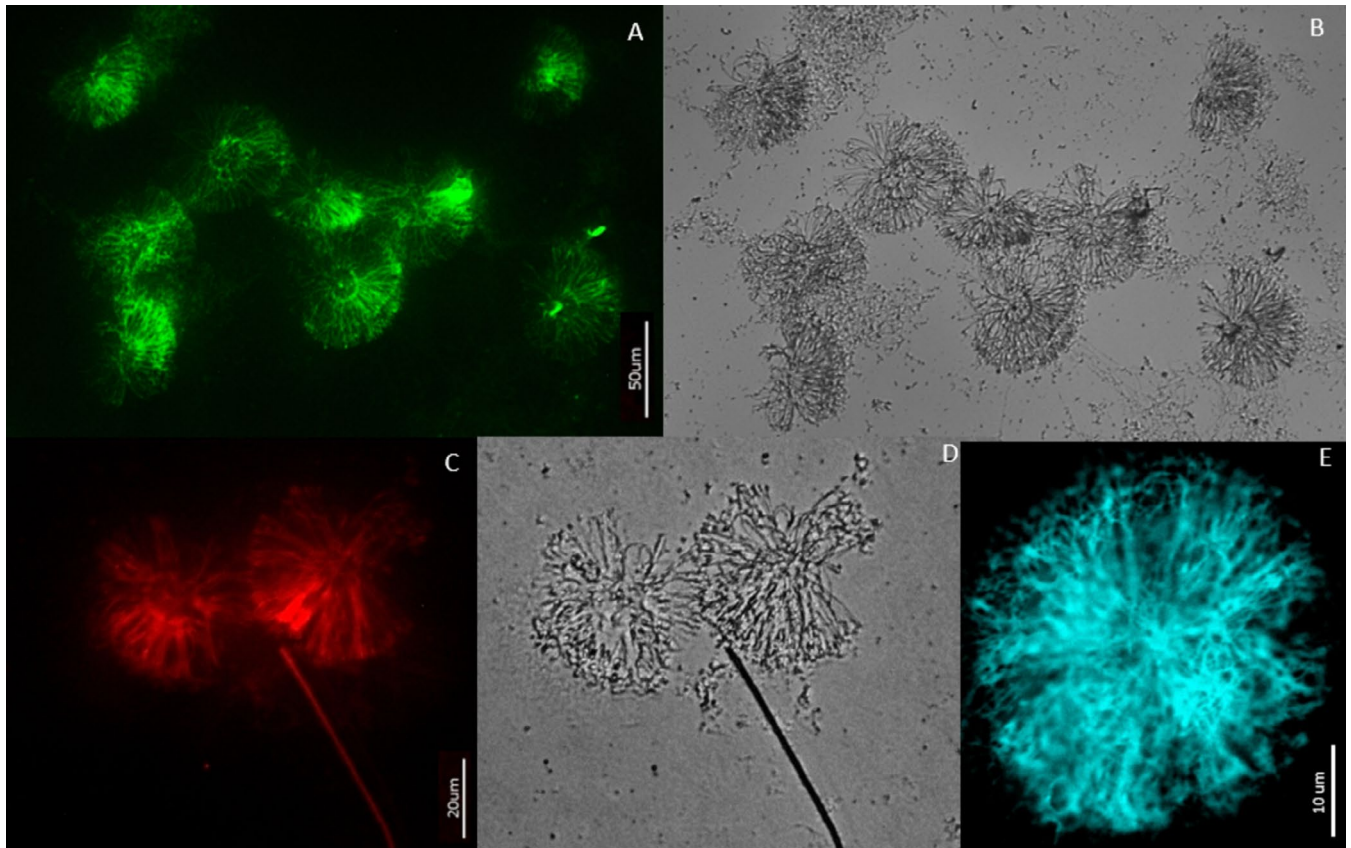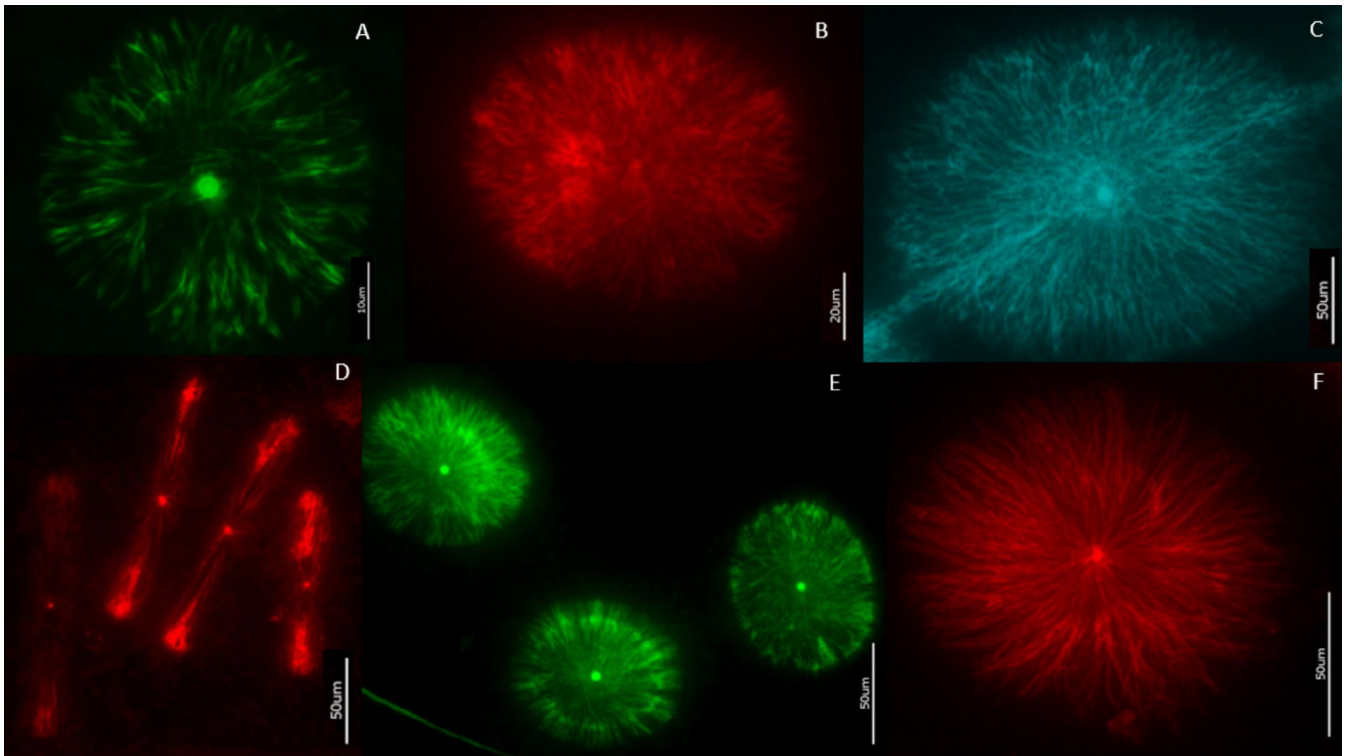
FIGURE 5 | Fluorescence microscopy of *G. cydonium* demineralized sterrasters stained with phalloidin: (A, B) 488-phalloidin; (C, D) 594-phalloidin; (E) 350-phalloidin, oil immersion lens. (A, C, E) were made using Ex/Em 470/525, 560/630, and 360/460 nm, respectively, (B, D) were made with the bright field condition.
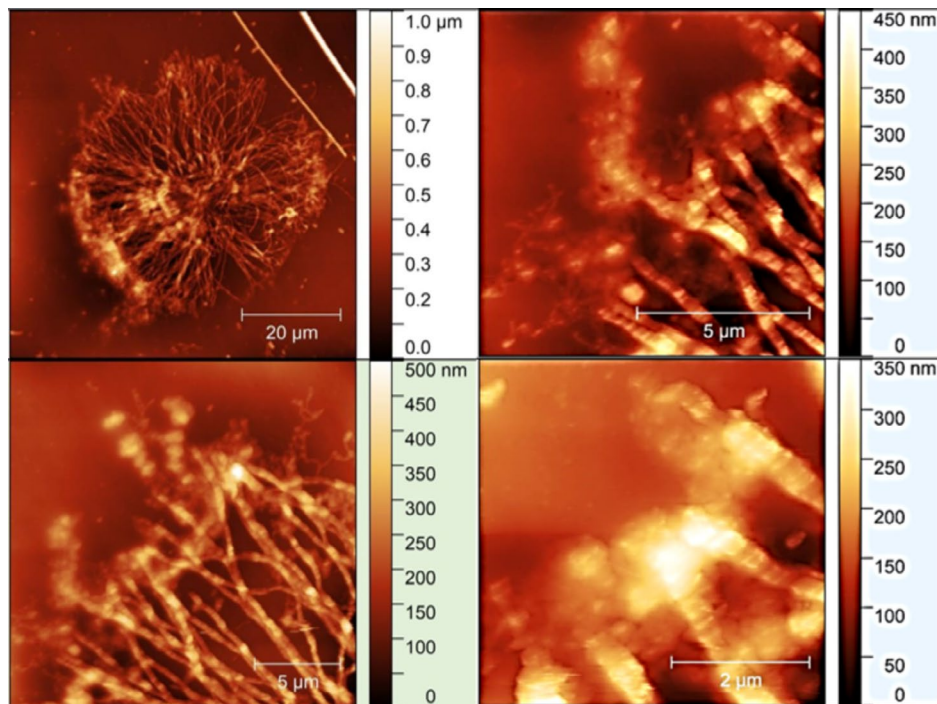
FIGURE 6 | AFM at four different scales of the axial filaments after *G. cydonium* sterrasters desilicification.

been reported in other important sponge biosilicification molecules such as chitins (Ehrlich et al. 2016), collagens (Ehrlich et al. 2010), silicateins, glassins, and related proteins (Shimizu et al. 2024; Wysokowski, Jesionowski, and Ehrlich 2018). For comparison, the actin bundles in bristle sprouts of *Drosophila* fruit flies contain 500 filaments (Tilney, Tilney,

FIGURE 7 | Fluorescence microscopy of phalloidin-stained sterrasters of sponges belonging to subfamily Erylinae: (A) *Caminella intuta*, (B) *Caminus vulcani*, (C) *Pachymatisma normani*, (D) *Erylus formosus*, (E) *Erylus euastrum*, and (F) *Erylus granularis*.
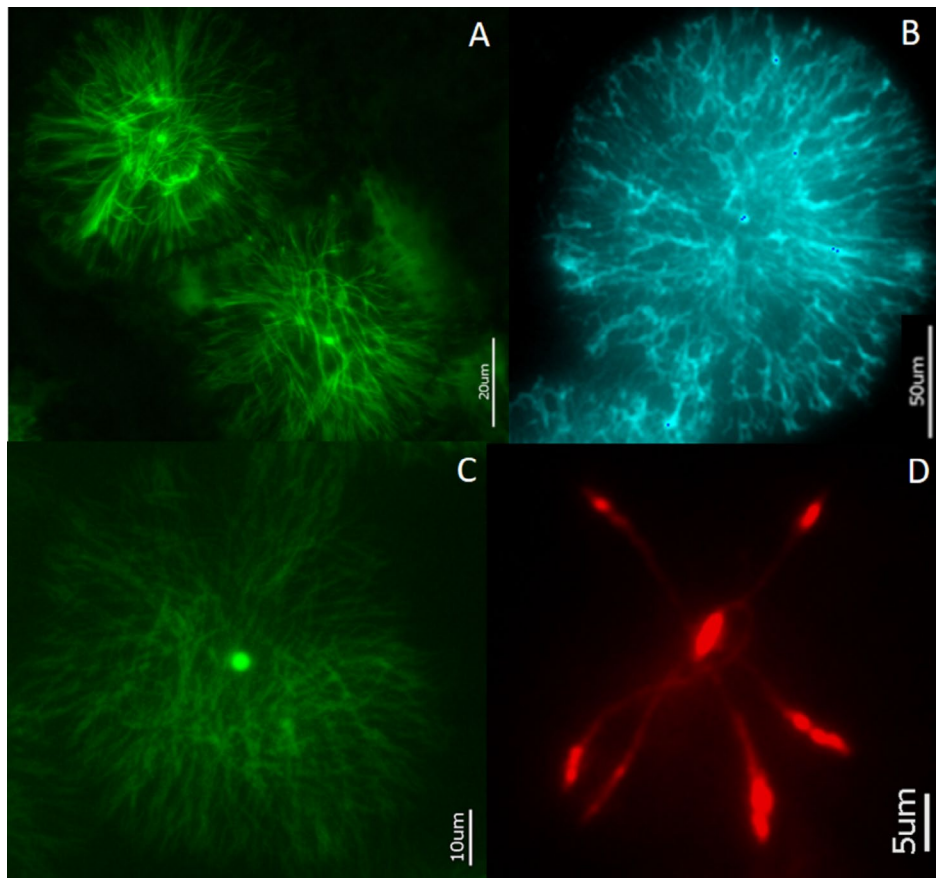
FIGURE 8 | Fluorescence microscopy of phalloidin-stained sterrasters of sponges belonging to subfamily Geodiinae: (A) *Geodia barretti*, (B) *Geodia macandrewii*, (C) *Geodia phlegraei*, and (D) *Rhabdastrella globostellata*.

and Guild 1995). Actin filaments longer than 5 μm long are not exceptional (Takatsuki, Bengtsson, and Månsson 2014). For example, in stereocilia, filopodia, and stress fibers, the length of actin filaments reaches several dozens of micrometers (Rajan, Kudryashov, and Reisler 2023). In *Drosophila*, the long bristle cell extension is supported by equally long (up to 400 μm) actin filament bundles assembled together (Guild et al. 2005; Tilney et al. 2000).

Observation of actin bundles within sterrasters is not surprising due to the well-known ability of actin to form double-stranded helical filaments with a tendency to self-assembly (Pollard, Blanchoin, and Mullins 2000) into higher-order suprafilamentous 3D constructs (i.e., bundles, branched networks, crosslinked and dendritic filament networks, as well as aggregates) (Castaneda, Park, and Kang 2021; Chen et al. 2023; Martiel et al. 2020). Despite the modern view (Chen et al. 2023) that the assembly of actin filaments into higher-order structures depends on enthalpic interactions between actin filaments and both biological (i.e., 13 distinct actin-binding proteins) and chemical crosslinks as well as a number of physical interactions (i.e., counterion condensation, steric confinement, shear forces, Van der Waals attraction), the mechanisms of growth, and differentiation of poriferan actin filaments of spicular origin remain unknown.

The same fluorescent technique as for *G. cydonium* (Figure 5) was also used for the other geodiid sponges from the Erylinae subfamily (*Caminella intuta*, *Caminus vulcani*, *Erylus euastrum*, *Erylus formosus*, *Erylus granularis*, *Pachymatisma normani*) (Figure 7A–F) and Geodiinae subfamily (*G. barretti*, *G. macandrewii*, *G. phlegraei*) (Figure 8A–C) as well as for *Rhabdastrella globostellata* (Figure 8D), which may belong to the genus *Geodia* based on molecular analysis (Cárdenas et al. 2011). All samples have shown strong fluorescence confirming actin presence in the axial filaments of their sterrasters.

One common feature for all actin filaments of sterrasters under study is their radially oriented organization within corresponding sphere-like bundles (Figures 5–8). This radial structural orientation has already been reported for both intracellular and extracellular actins. Thus, more than 5-μm-long radial actin bundles have been previously found in the growth cone of *Aplysia* bag cell neurons (Katoh et al. 1999a, 1999b), lamellipodia of motile cells (Danuser and Oldenbourg 2000), neuronal growth cones (Oldenbourg, Katoh, and Danuser 2000), flagella (Pochitaloff et al. 2022), filopodia (Schaefer, Kabir, and Forscher 2002), *Drosophila* S2 cells, as well as *Xenopus* XTC cells (Belin, Goins, and Mullins 2014). Also, the radial pattern of cortical actin filaments has been reported in *Arabidopsis* plant guard cells of dark-closed stomata (Eun and Lee 1997; Li et al. 2019). In humans, the presence of large F-actin aggregates in the extracellular matrix in the nucleus pulposus tissue of patients with discogenic dorsopathy has been reported (Sudakov et al. 2017). These aggregates were several times larger than the neutrophils and chondrocytes within the necrosis area and consisted of radially oriented actin filaments.

The creation of the principal radial actin model is actively researched at present (Chandrasekaran, Upadhyaya, and

Papoian 2019). For example, it was shown that in cultured rodent neurons centrosomes serve as a radial actin-organizing center (Meka et al. 2019). Moreover, highly special F-actin aster-like structures in these cells have been visualized using superresolution microscopy and live-cell imaging. Also, in the case of siliceous frustules of such large size diatom as *Coscinodiscus granii*, the presence of radially oriented actin-based filamentous matrix has been reported previously (Tesson and Hildebrand 2010).

Intriguingly, actin-organizing centers are particularly visible on our fluorescence microscopy images (Figures 5, 7, and 8) due to their intense fluorescence after phalloidin-based staining. Further investigations on the origin and nanostructural organization of such centers responsible for actin radial organization in sterrasters should be carried out. Close to the center, an inner circular structure more or less diffuse is also often revealed with fluorescence (Figure 7C) in *Pachymatisma* and *Geodia* species suggesting that there may be a second organizing structure, whose function is unknown at this point. This secondary structure may reflect the border of the central cavity found in some sterrasters (Cárdenas and Rapp 2013; figs 2-1, 2-2, and 2-4 in Rützler and Macintyre 1978). A similar structure is observed with Coomassie brilliant blue staining of sterrasters (see fig 6B,C in Müller et al. 2007). Since the large star-shaped spicules of *R. globostellata* have few branches, it is expected to see only a handful of actin filaments (Figure 8D). However, the terminal part of these filaments is significantly brighter suggesting a higher density of actin, a feature not observed in the sterrasters.

What are the limiting factors for the size and length of spicules like sterrasters? For example, in *Drosophila* bristle cells, it was shown that the actin filament bundles disappear once the actin-containing bristle elongates to its mature length. Simultaneously, the bristle cell shape is maintained by the chitinous exoskeletal layer (Tilney, Tilney, and Guild 1995). In poriferan biosilica, the actin remains in the axial filaments within already formed sterrasters and similar constructs. This phenomenon is also an open question. The proteinaceous axial filament is formed generally from the actin which does not undergo mineralization itself and can grow from the distal part of the spicule branch. This process continues as long as the top of the ray is opened and stops when the top of the spicule is covered by silica deposition. Thus the actin together with the final enclosure of the spicule top could provide not only the spicule shape but also the final spicule size.

No major structural actin differences were observed between the spherical sterrasters of *Geodia* (Figure 8) and the flattened sterrasters (= aspidasters) of *Erylus* (Figure 7D–F), nor more largely between the Geodiinae (Figure 8) and the Erylinae species (Figure 7). Molecular phylogenetic data suggest that sterrasters may have appeared in spicule evolution at least three times independently (Cárdenas 2020): in the Geodiinae, in the Erylinae, and in *Caminella*. The present results show that an apparent similar axial filament and actin general structure is used for these different sterrasters suggesting an actin process common to the whole geodiid family, and therefore already present at the emergence of the family (~170 million years ago). The surface microornamentation differences observed in the different genera have other origins, probably involving

processes during the surface secondary silicification. Since our 10% HF treatment dissolves the surface rosettes, the microfilaments from which they originate are probably lost in the process since they do not seem to be connected to the main polyaxial filament structure (see figs 2 and 3 in Rützler and Macintyre 1978). Additional protocols will be needed to image the potential presence of actin on the surface of sterrasters and thus test their role in the surface microornamentation patterning.

Recently, F-actins isolated from diverse biosilica structures of selected representatives of such poriferan classes as Hexactinellida, Demospongiae, and Homoscleromorpha obtained the common term "Silactins" (Ehrlich et al. 2024). It should be noted that the identification of silactins within spicules of *Plakortis halihondrioides* and *Plakina jamaicensis*, which belong to homoscleromorphs, has been reported for the first time. It is hoped that silactins, so far undeservedly overlooked by the scientific community in relation to poriferan biosilica, will now become a focus of detailed investigations. For example, both common as well as individual structural and functional features of silactins with respect to species-specific morphologies should be studied in near future.

4 | Conclusions

Our study confirms actin in a recently discovered role: patterning biosilica microscleres of demosponges in vivo on an example of 11 different geodiid species. All geodiid sterrasters share a common polyaxial radial actin network with a clear center and a possible secondary structure. No major actin network differences were observed between the different geodiid genera or subfamilies. The most interesting feature is the presence of apparent multifilament aggregates with a well-defined periodicity observed in our *G. cydonium* sterrasters axial filaments AFM images (Figure 6). Further studies on the principles of the nano- and microstructural organization of these sterraster radial actin filaments are necessary, although represent a challenging methodological task.

Author Contributions

Alona Voronkina: writing – original draft, investigation, visualization. **Paco Cárdenas:** writing – original draft, validation, resources, supervision, writing – review and editing, visualization. **Jörg Adam:** investigation. **Heike Meissner:** investigation. **Krzysztof Nowacki:** investigation, visualization. **Yvonne Joseph:** methodology, supervision. **Konstantin R. Tabachnick:** conceptualization, investigation, writing – review and editing. **Hermann Ehrlich:** conceptualization, methodology, resources, writing – original draft, visualization, supervision, funding acquisition, writing – review and editing.

Conflicts of Interest

The authors declare no conflicts of interest.

References

Belin, B. J., L. M. Goins, and R. D. Mullins. 2014. "Comparative Analysis of Tools for Live Cell Imaging of Actin Network Architecture." *BioArchitecture* 4: 189–202. https://doi.org/10.1080/19490992.2014.1047714.

Buchwalow, I., V. Samoilova, W. Boecker, and M. Tiemann. 2011. "Non-Specific Binding of Antibodies in Immunohistochemistry: Fallacies and Facts." *Scientific Reports* 1: 28. https://doi.org/10.1038/srep00028.

Cano, M. L., L. Cassimeris, M. Fechheimer, and S. H. Zigmond. 1992. "Mechanisms Responsible for F-Actin Stabilization After Lysis of Polymorphonuclear Leukocytes." *Journal of Cell Biology* 116: 1123–1134. https://doi.org/10.1083/jcb.116.5.1123.

Cárdenas, P. 2020. "Surface Microornamentation of Demosponge Sterraster Spicules, Phylogenetic and Paleontological Implications." *Frontiers in Marine Science* 7: 613610. https://doi.org/10.3389/fmars.2020.613610.

Cárdenas, P., and H. T. Rapp. 2013. "Disrupted Spiculogenesis in Deep-Water Geodiidae (Porifera, Demospongiae) Growing in Shallow Waters." *Invertebrate Biology* 132: 173–194. https://doi.org/10.1111/ivb.12027.

Cárdenas, P., H. T. Rapp, A. B. Klitgaard, M. Best, M. Thollesson, and O. S. Tendal. 2013. "Taxonomy, Biogeography and DNA Barcodes of Geodia Species (Porifera, Demospongiae, Tetractinellida) in the Atlantic Boreo-Arctic Region: Revision of Atlantic Boreo-Arctic Geodia." *Zoological Journal of the Linnean Society* 169, no. 2: 251–311. https://doi.org/10.1111/zoj.12056.

Cárdenas, P., H. T. Rapp, C. Schander, and O. S. Tendal. 2010. "Molecular Taxonomy and Phylogeny of the Geodiidae (Porifera, Demospongiae, Astrophorida)–Combining Phylogenetic and Linnaean Classification." *Zoologica Scripta* 39: 89–106. https://doi.org/10.1111/j.1463-6409.2009.00402.x.

Cárdenas, P., J. R. Xavier, J. Reveillaud, C. Schander, and H. T. Rapp. 2011. "Molecular Phylogeny of the Astrophorida (Porifera, Demospongiaep) Reveals an Unexpected High Level of Spicule Homoplasy." *PLoS One* 6: e18318. https://doi.org/10.1371/journal.pone.0018318.

Castaneda, N., J. Park, and E. H. Kang. 2021. "Regulation of Actin Bundle Mechanics and Structure by Intracellular Environmental Factors." *Frontiers of Physics* 9: 675885. https://doi.org/10.3389/fphy.2021.675885.

Chandrasekaran, A., A. Upadhyaya, and G. A. Papoian. 2019. "Remarkable Structural Transformations of Actin Bundles Are Driven by Their Initial Polarity, Motor Activity, Crosslinking, and Filament Treadmilling." *PLoS Computational Biology* 15: e1007156. https://doi.org/10.1371/journal.pcbi.1007156.

Chang, S., L. Zhang, S. Clausen, D. J. Bottjer, and Q. Feng. 2019. "The Ediacaran-Cambrian Rise of Siliceous Sponges and Development of Modern Oceanic Ecosystems." *Precambrian Research* 333: 105438. https://doi.org/10.1016/j.precamres.2019.105438.

Chen, X., S. J. Roeters, F. Cavanna, J. Alvarado, and C. R. Baiz. 2023. "Crowding Alters F-Actin Secondary Structure and Hydration." *Communications Biology* 6: 1–12. https://doi.org/10.1038/s42003-023-05274-3.

Danuser, G., and R. Oldenbourg. 2000. "Probing f-Actin Flow by Tracking Shape Fluctuations of Radial Bundles in Lamellipodia of Motile Cells." *Biophysical Journal* 79: 191–201. https://doi.org/10.1016/S0006-3495(00)76283-7.

Dhakal, K., B. Black, and S. Mohanty. 2014. "Introduction of Impermeable Actin-Staining Molecules to Mammalian Cells by Optoporation." *Scientific Reports* 4: 6553. https://doi.org/10.1038/srep06553.

Ehrlich, H., E. Brunner, P. Simon, et al. 2011. "Calcite Reinforced Silica-Silica Joints in the Biocomposite Skeleton of Deep-Sea Glass Sponges." *Advanced Functional Materials* 21: 3473–3481. https://doi.org/10.1002/adfm.201100749.

Ehrlich, H., R. Deutzmann, E. Brunner, et al. 2010. "Mineralization of the Metre-Long Biosilica Structures of Glass Sponges Is Templated on Hydroxylated Collagen." *Nature Chemistry* 2: 1084–1088. https://doi.org/10.1038/nchem.899.

Ehrlich, H., M. Luczak, R. Ziganshin, et al. 2022. "Arrested in Glass: Actin Within Sophisticated Architectures of Biosilica in Sponges." *Advanced Science* 9: 2105059. https://doi.org/10.1002/ADVS.202105059.

Ehrlich, H., M. Maldonado, A. R. Parker, et al. 2016. "Supercontinuum Generation in Naturally Occurring Glass Sponges Spicules." *Advanced Optical Materials* 4: 1608–1613. https://doi.org/10.1002/adom.201600454.

Ehrlich, H., A. Voronkina, K. Tabachnick, A. Kubiak, A. Ereskovsky, and T. Jesionowski. 2024. "Silactins and Structural Diversity of Biosilica in Sponges." *Biomimetics* 9, no. 7: 393. https://doi.org/10.3390/biomimetics9070393.

Eun, S. O., and Y. Lee. 1997. "Actin Filaments of Guard Cells Are Reorganized in Response to Light and Abscisic Acid." *Plant Physiology* 115: 1491–1498. https://doi.org/10.1104/pp.115.4.1491.

Gilmore, J. L., M. Kumeta, and K. Takeyasu. 2013. "AFM Investigation of the Organization of Actin Bundles Formed by Actin-Binding Proteins." *Journal of Surface Engineered Materials and Advanced Technology* 03: 13–19. https://doi.org/10.4236/jsemat.2013.34a1002.

Görlich, S., A. J. Samuel, R. J. Best, et al. 2020. "Natural Hybrid Silica/Protein Superstructure at Atomic Resolution." *Proceedings of the National Academy of Sciences of the United States of America* 117: 31088–31093. https://doi.org/10.1073/pnas.2019140117.

Guild, G. M., P. S. Connelly, L. Ruggiero, K. A. Vranich, and L. G. Tilney. 2005. "Actin Filament Bundles in Drosophila Wing Hairs: Hairs and Bristles Use Different Strategies for Assembly." *Molecular Biology of the Cell* 16: 3620–3631. https://doi.org/10.1091/mbc.E05-03-0185.

Han, Y., S. Tu, W. Gong, et al. 2023. "Three-Dimensional Multi-Color Optical Nanoscopy at Sub-10-Nm Resolution Based on Small-Molecule Organic Probes." *Cell Reports Methods* 3, no. 9: 100556. https://doi.org/10.1016/j.crmeth.2023.100556.

Henderson, E., P. G. Haydon, and D. S. Sakaguchi. 1992. "Actin Filament Dynamics in Living Glial Cells Imaged by Atomic Force Microscopy." *Science* 257, no. 5078: 1944–1946. https://doi.org/10.1126/science.1411511.

Henderson, E., and D. S. Sakaguchi. 1993. "Imaging F-Actin in Fixed Glial Cells With a Combined Optical Fluorescence/Atomic Force Microscope." *NeuroImage* 1: 145–150. https://doi.org/10.1006/nimg.1993.1007.

Jung, M., D. Kim, and J. Y. Mun. 2020. "Direct Visualization of Actin Filaments and Actin-Binding Proteins in Neuronal Cells." *Frontiers in Cell and Developmental Biology* 8: 588556. https://doi.org/10.3389/fcell.2020.588556.

Katoh, K., K. Hammar, P. J. S. Smith, and R. Oldenbourg. 1999a. "Arrangement of Radial Actin Bundles in the Growth Cone of Aplysia Bag Cell Neurons Shows the Immediate Past History of Filopodial Behavior." *Proceedings of the National Academy of Sciences of the United States of America* 96: 7928–7931. https://doi.org/10.1073/pnas.96.14.7928.

Katoh, K., K. Hammar, P. J. S. Smith, and R. Oldenbourg. 1999b. "Birefringence Imaging Directly Reveals Architectural Dynamics of Filamentous Actin in Living Growth Cones." *Molecular Biology of the Cell* 10: 197–210. https://doi.org/10.1091/mbc.10.1.197.

Klitgaard, A. B., and O. S. Tendal. 2004. "Distribution and Species Composition of Mass Occurrences of Large-Sized Sponges in the Northeast Atlantic." *Progress in Oceanography* 61: 57–98. https://doi.org/10.1016/j.pocean.2004.06.002.

Li, X., M. Diao, Y. Zhang, G. Chen, S. Huang, and N. Chen. 2019. "Guard Cell Microfilament Analyzer Facilitates the Analysis of the Organization and Dynamics of Actin Filaments in Arabidopsis Guard Cells." *International Journal of Molecular Sciences* 20: 2753. https://doi.org/10.3390/ijms20112753.

Łukowiak, M. 2020. "Utilizing Sponge Spicules in Taxonomic, Ecological and Environmental Reconstructions: A Review." *PeerJ* 8: e10601. https://doi.org/10.7717/peerj.10601.

Łukowiak, M., R. Van Soest, M. Klautau, T. Pérez, A. Pisera, and K. Tabachnick. 2022. "The Terminology of Sponge Spicules." *Journal of Morphology* 283: 1517–1545. https://doi.org/10.1002/jmor.21520.

Martiel, J. L., A. Michelot, R. Boujemaa-Paterski, L. Blanchoin, and J. Berro. 2020. "Force Production by a Bundle of Growing Actin Filaments Is Limited by Its Mechanical Properties." *Biophysical Journal* 118: 182–192. https://doi.org/10.1016/j.bpj.2019.10.039.

Meka, D. P., R. Scharrenberg, B. Zhao, et al. 2019. "Radial Somatic F-Actin Organization Affects Growth Cone Dynamics During Early Neuronal Development." *EMBO Reports* 20, no. 12: e47743. https://doi.org/10.15252/embr.201947743.

Melak, M., M. Plessner, and R. Grosse. 2017. "Actin Visualization at a Glance." *Journal of Cell Science* 130: 525–530. https://doi.org/10.1242/jcs.189068.

Moreno, B., A. DiCorato, A. Park, et al. 2019. "Culture of and Experiments With Sea Urchin Embryo Primary Mesenchyme Cells." *Methods in Cell Biology* 150: 293–330. https://doi.org/10.1016/bs.mcb.2019.01.002.

Müller, W. E. G., U. Schloßmacher, C. Eckert, et al. 2007. "Analysis of the Axial Filament in Spicules of the Demosponge *Geodia cydonium*: Different Silicatein Composition in Microscleres (Asters) and Megascleres (Oxeas and Triaenes)." *European Journal of Cell Biology* 86: 473–487. https://doi.org/10.1016/j.ejcb.2007.06.002.

Narita, A., E. Usukura, A. Yagi, et al. 2016. "Direct Observation of the Actin Filament by Tip-Scan Atomic Force Microscopy." *Microscopy* 65: 370–377. https://doi.org/10.1093/jmicro/dfw017.

Oldenbourg, R., K. Katoh, and G. Danuser. 2000. "Mechanism of Lateral Movement of Filopodia and Radial Actin Bundles Across Neuronal Growth Cones." *Biophysical Journal* 78: 1176–1182. https://doi.org/10.1016/S0006-3495(00)76675-6.

Pisera, A. 2003. "Some Aspects of Silica Deposition in Lithistid Demosponge Desmas." *Microscopy Research and Technique* 62: 312–326. https://doi.org/10.1002/jemt.10398.

Pochitaloff, M., M. Miranda, M. Richard, et al. 2022. "Flagella-Like Beating of Actin Bundles Driven by Self-Organized Myosin Waves." *Nature Physics* 18: 1240–1247. https://doi.org/10.1038/s41567-022-01688-8.

Pollard, T. D., L. Blanchoin, and R. D. Mullins. 2000. "Molecular Mechanisms Controlling Actin Filament Dynamics in Nonmuscle Cells." *Annual Review of Biophysics and Biomolecular Structure* 29: 545–576. https://doi.org/10.1146/annurev.biophys.29.1.545.

Pospich, S., F. Merino, and S. Raunser. 2020. "Structural Effects and Functional Implications of Phalloidin and Jasplakinolide Binding to Actin Filaments." *Structure* 28: 437–449.e5. https://doi.org/10.1016/j.str.2020.01.014.

Rajan, S., D. S. Kudryashov, and E. Reisler. 2023. "Actin Bundles Dynamics and Architecture." *Biomolecules* 13: 450. https://doi.org/10.3390/biom13030450.

Romani, M., and J. Auwerx. 2021. "Phalloidin Staining of Actin Filaments for Visualization of Muscle Fibers in *Caenorhabditis elegans*." *Bio-Protocol* 11: e4183. https://doi.org/10.21769/BIOPROTOC.4183.

Rützler, K., and I. G. Macintyre. 1978. "Siliceous Sponge Spicules in Coral Reef Sediments." *Marine Biology* 49, no. 2: 147–159. https://doi.org/10.1007/BF00387114.

Schaefer, A. W., N. Kabir, and P. Forscher. 2002. "Filopodia and Actin Arcs Guide the Assembly and Transport of Two Populations of Microtubules With Unique Dynamic Parameters in Neuronal Growth Cones." *Journal of Cell Biology* 158: 139–152. https://doi.org/10.1083/jcb.200203038.

Schoeppler, V., E. Reich, J. Vacelet, et al. 2017. "Shaping Highly Regular Glass Architectures: A Lesson From Nature." *Science Advances* 3: eaao2047. https://doi.org/10.1126/sciadv.aao2047.

Shao, Z., D. Shi, and A. V. Somlyo. 2000. "Cryoatomic Force Microscopy of Filamentous Actin." *Biophysical Journal* 78: 950–958. https://doi.org/10.1016/S0006-3495(00)76652-5.

Shimizu, K., T. Amano, M. R. Bari, J. C. Weaver, J. Arima, and N. Mori. 2015. "Glassin, a Histidine-Rich Protein From the Siliceous Skeletal System of the Marine Sponge Euplectella, Directs Silica Polycondensation." *Proceedings of the National Academy of Sciences of the United States of America* 112: 11449–11454. https://doi.org/10.1073/PNAS.1506968112.

Shimizu, K., M. Nishi, Y. Sakate, et al. 2024. "Silica-Associated Proteins From Hexactinellid Sponges Support an Alternative Evolutionary Scenario for Biomineralization in Porifera." *Nature Communications* 15: 181. https://doi.org/10.1038/s41467-023-44226-7.

Simpson, T. L. 1989. "Silicification Processes in Sponges: Geodia Asters and the Problem of Morphogenesis of Spicule Shape." In *Origin, Evolution, and Modern Aspects of Biomineralization in Plants and Animals*. Boston, MA: Springer. https://doi.org/10.1007/978-1-4757-6114-6_9.

Sollas, W. J. 1880. "The Sponge-Fauna of Norway; a Report on the Rev. A. M. Norman's Collection of Sponges From the Norwegian Coast." *Annals and Magazine of Natural History* 5, no. 27: 241–259. https://doi.org/10.1080/00222938009459417.

Sudakov, N. P., I. V. Klimenkov, V. A. Byvaltsev, S. B. Nikiforov, and Y. M. Konstantinov. 2017. "Extracellular Actin in Health and Disease." *Biokhimiia* 82, no. 1: 1–12. https://doi.org/10.1134/S0006297917010011.

Takatsuki, H., E. Bengtsson, and A. Månsson. 2014. "Persistence Length of Fascin-Cross-Linked Actin Filament Bundles in Solution and the In Vitro Motility Assay." *Biochimica et Biophysica Acta* 1840, no. 6: 1933–1942. https://doi.org/10.1016/j.bbagen.2014.01.012.

Tesson, B., and M. Hildebrand. 2010. "Extensive and Intimate Association of the Cytoskeleton With Forming Silica in Diatoms: Control Over Patterning on the Meso- and Micro-Scale." *PLoS One* 5, no. 12: e14300. https://doi.org/10.1371/journal.pone.0014300.

Tilney, L. G., P. S. Connelly, K. A. Vranich, M. K. Shaw, and G. M. Guild. 2000. "Regulation of Actin Filament Cross-Linking and Bundle Shape in Drosophila Bristles." *Journal of Cell Biology* 148: 87–99. https://doi.org/10.1083/jcb.148.1.87.

Tilney, L. G., M. S. Tilney, and G. M. Guild. 1995. "F Actin Bundles in Drosophila Bristles I. Two Filament Cross-Links Are Involved in Bundling." *Journal of Cell Biology* 130: 629–638. https://doi.org/10.1083/jcb.130.3.629.

Uriz, M. J., X. Turon, M. A. Becerro, and G. Agell. 2003. "Siliceous Spicules and Skeleton Frameworks in Sponges: Origin, Diversity, Ultrastructural Patterns, and Biological Functions." *Microscopy Research and Technique* 62: 279–299. https://doi.org/10.1002/jemt.10395.

Voronkina, A., E. Romanczuk-Ruszuk, R. E. Przekop, et al. 2023. "Honeycomb Biosilica in Sponges: From Understanding Principles of Unique Hierarchical Organization to Assessing Biomimetic Potential." *Biomimetics* 8: 234. https://doi.org/10.3390/biomimetics8020234.

Wang, X., M. Wiens, H. C. Schröder, et al. 2010. "Morphology of Sponge Spicules: Silicatein a Structural Protein for Bio-Silica Formation." *Advanced Engineering Materials* 12, no. 9: B422–B437. https://doi.org/10.1002/adem.200980042.

Wysokowski, M., T. Jesionowski, and H. Ehrlich. 2018. "Biosilica as a Source for Inspiration in Biological Materials Science." *American Mineralogist* 103: 665–691. https://doi.org/10.2138/am-2018-6429.

Zhang, J., Y. L. Wang, L. Gu, and J. Pan. 2003. "Atomic Force Microscopy of Actin." *Acta Biochimica et Biophysica Sinica Shanghai* 35, no. 6: 489–494.